

Antifungal Evaluation of Copper(II) Complex from a Schiff Base Derivative of Pyrazine on *Schizosaccharomyces pombe*^①

YANG Ping^②

(School of Environment, Jinan University, Guangzhou 511443, China)

ABSTRACT A new copper(II) complex of CuLCl_2 , where $\text{L} = \text{N}^1$ -(1-pyrazin-2-yl-ethylidene)-ethane-1,2-diamine, a tridentate Schiff base derived from 2-acetylpyrazine has been prepared. The complex has been characterized by FT-IR, elemental analysis and single-crystal X-ray diffraction studies. Structural studies reveal that CuLCl_2 is a mononuclear copper(II) complex with distorted square pyramidal geometry. Antifungal activity of CuLCl_2 was investigated by use of microcalorimetric measurement system and evaluated against *S. pombe*. It has high antifungal activity with $IC_{50} = 213 \mu\text{g/mL}$.

Keywords: antifungal agents, copper, Schiff bases, pyrazine, *S. pombe*;

DOI: 10.14102/j.cnki.0254-5861.2011-2084

1 INTRODUCTION

In the past few decades, the fungal infections have increased at an alarming rate in the world^[1-3]. They possess severe threats to human health. For example, *Candida albicans* is responsible for mucosal and cutaneous infections^[4, 5] and it can cause vaginitis, oral thrush and athlete's foot. *Cryptococcus neoformans* can lead to disease in apparently immunocompetent, as well as immune-compromised, hosts^[6]. It is best known for causing a severe form of meningitis and meningo-encephalitis in people with HIV/AIDS^[7]. In addition, naturally fungal disease has drug resistance, so medical field is in a constant state to invent new drugs to treat these kinds of problems.

Schiff bases and its complexes constitute an important class of biologically active drug molecules, which have attracted attention of chemists due to their wide range of pharmacological properties^[8, 9].

They are widely used in the development of anti-proliferative^[10], antibacterial^[11] and antifungal drugs^[12-14]. Among these, copper(II) is especially attractive due to its capability of assuming different shapes with different coordination numbers and its redox property. In some cases, the pharmacological activity of Cu(II) complexes was found to be much higher than that of the ligands alone and other metal coordination compounds^[15-17].

In this work, we described the synthesis and characterization of a copper(II) complex (CuLCl_2) of the ligand N^1 -(1-Pyrazin-2-yl-ethylidene)-ethane-1,2-diamine (L). The ligand was selected because it has multidentate sites and can form five- or six-membered chelate ring with metals, which was expected to increase the stability of its complexes in solution. *Schizosaccharomyces pombe* (*S. pombe*) is a species of yeast used in traditional brewing and as a model organism in molecular and cell biology^[18, 19]. It is a unicellular eukaryote distantly related to

Received 28 May 2018; accepted 17 August 2018 (CCDC 1035998)

① This work was supported by the National Natural Science Foundation of China (No. 41701349)

② Corresponding author. Yang Ping, doctor, majoring in coordination chemistry. E-mail: 191723030@qq.com

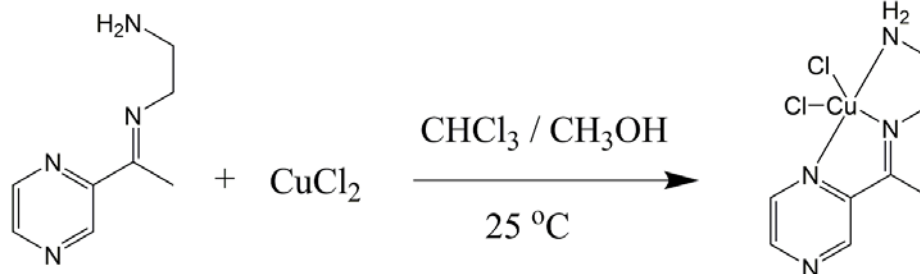
pathogenic microorganism *C. neoformans*^[20]. Therefore, the antifungal activity of the synthesized complex was tested in vitro with *S. pombe*.

2 EXPERIMENTAL

2.1 Material and methods

The reagents and solvents were commercially available without any further purification. The C, H, and N microanalyses were carried out with a Vario EL elemental analyzer. Fourier transform infrared (FT-IR) spectra were recorded from KBr pellets in the range of 400 ~ 4000 cm^{-1} on a Nicolet Avatar 360 spectrometer. Electron spray ionization (ESI) mass spectra were obtained on a LCQ DECA XP quadrupole ion trap mass spectrometer with methanol as a carrier solvent. Powder X-ray diffraction (PXRD) patterns were recorded on an Empyrean diffractometer with $\text{CuK}\alpha$ radiation ($\lambda = 1.5406 \text{ \AA}$) at an increment of 0.02° and scanning rate of $4^\circ/\text{min}$ with 2θ ranging from 5 to 50° .

2.2 Synthesis of Schiff base copper



Scheme 1. Synthetic reaction formula of the complex

2.3 X-ray crystallography

Diffraction intensities for the complex were collected on a CrysAlisPro Agilent Technologies diffractometer with mirror-monochromator $\text{CuK}\alpha$ radiation ($\lambda = 1.5418 \text{ \AA}$). Empirical absorption correction using spherical harmonics, implemented in SCALE3 ABSPACK scaling algorithm. The structures were solved by direct methods and refined with full-matrix least-squares technique using SHELXS-97 and SHELXL-97 programs, respectively. Anisotropic thermal parameters were applied to all non-hydrogen atoms. The organic hydrogen atoms were generated geometrically (methyl C–H

complex (CuLCl_2)

2-Acetylpyrazine (10 mmol, 1.22 g) was slowly added to an absolute ethanol (20 mL) of ethylene diamine (15 mmol, 0.9 g). The mixture was heated under reflux with stirring for 2 h. Then the solution was slowly evaporating for a week at room temperature. After a large light yellow crystal of the N^1 -(1-pyrazin-2-yl-ethylidene)-ethane-1,2-diamine (**L**) was obtained, 0.2 mmol (32.8 mg) of **L** in 15 mL of chloroform and 0.2 mmol (27.2 mg) of CuCl_2 in 10 mL of methanol were mixed and stirred at room temperature for 0.5 h. After filtering, the filtrate is free evaporation. Blue block-shaped single crystals of the title complex (CuLCl_2) suitable for X-ray diffraction analysis were obtained after two weeks (yield 58% based on Cu). The synthetic reaction formula is shown in Scheme 1. Calcd. for $\text{C}_8\text{H}_{12}\text{N}_4\text{Cl}_2\text{Cu}$: C, 32.11; H, 4.01; N, 18.73%. Found: C, 32.54; H, 4.05; N, 18.72%. FT-IR data (KBr pellet, cm^{-1}): 3290 s, 3235 s, 1658 s, 1565 m, 1411 s, 1373 m, 1304 m, 1182 s, 1109 m, 1040 s, 865 m, 788 w, 661 w, 538 w, 485 w, 454 m.

0.96 \AA , methylene C–H 0.97 \AA , pyrazinyl C–H 0.93 \AA , and N–H 0.90 \AA). Complex CuLCl_2 crystallizes in triclinic, space group $P\bar{1}$ with $a = 6.9064(5)$, $b = 8.8060(6)$, $c = 10.1255(6) \text{ \AA}$, $\alpha = 69.913(6)^\circ$, $\beta = 73.529(6)^\circ$, $\gamma = 83.682(6)^\circ$, $V = 554.56(6) \text{ \AA}^3$, $Z = 2$, $\text{Cu}(\text{C}_8\text{H}_{12}\text{N}_4)\text{Cl}_2$, $M_r = 298.66$, $D_c = 1.789 \text{ g/cm}^3$, $\mu = 6.985 \text{ mm}^{-1}$, $S = 1.075$, $F(000) = 302$, the final $R = 0.0364$ and $wR = 0.0998$ for 1811 observed reflections ($I > 2\sigma(I)$). $R_{\text{int}} = 0.0281$ (1931 independent reflections), $(\Delta\rho)_{\text{max}} = 0.522$ and $(\Delta\rho)_{\text{min}} = -0.961 \text{ e/\AA}^3$. Selected bond distances and bond angles are listed in Table 1.

Table 1. Selected Bond Lengths (Å) and Bond Angles (°) for CuLCl₂

Bond	Dist.	Bond	Dist.
Cu(1)–N(3)	1.981(2)	Cu(1)–N(4)	2.016(2)
Cu(1)–Cl(1)	2.2621(7)	Cu(1)–Cl(2)	2.4688(7)
Cu(1)–N(1)	2.056(2)		
Angle	(°)	Angle	(°)
N(3)–Cu(1)–N(4)	81.96(9)	N(3)–Cu(1)–N(1)	78.94(9)
N(3)–Cu(1)–Cl(1)	159.72(7)	N(4)–Cu(1)–Cl(1)	97.65(7)
N(3)–Cu(1)–Cl(2)	98.93(6)	N(4)–Cu(1)–Cl(2)	98.34(7)
Cl(1)–Cu(1)–Cl(2)	101.17(3)	N(4)–Cu(1)–N(1)	156.83(10)
N(1)–Cu(1)–Cl(2)	97.50(6)	N(1)–Cu(1)–Cl(1)	95.75(7)

2.4 Antifungal screening

2.4.1 *S. pombe* culture

Schizosaccharomyces pombe (*S. pombe*) was provided by Universidad de Salamanca and was cultivated in microbiological laboratory of Jinan University, Guangzhou, China. YES (yeast extract with supplement) culture medium contained 5 g yeast powder, 30 g glucose, 0.225 g leucine, 0.225 g adenine, 0.225 g lysine, 0.225 g uracil and 0.225 g histidine dissolving in 1000 mL of water which has undergone thrice distillation. Then, this culture medium was sterilized in highpressure steam for 30 min at the temperature of 121 °C. Initially, *S. pombe* was inoculated into 25 mL YES culture medium in 100 mL wide mouthed glass bottle and incubated in an oscillator for 8 h at 32 °C. Then, the freshly growing cells were diluted to 1×10^6 CFU/mL at the start of each experiment.

2.4.2 Microcalorimetric measurement

A TAM air eight-channel thermal conductivity isothermal microcalorimeter (Thermometric AB, Sweden) was used for microcalorimetric measurement. The thermal effect was observed in a hermetically closed 20 mL glass ampoule, which was sterilized at 121 °C prior to use. Initially, the density of *S. pombe* in YES culture medium was 1×10^6 colony forming units (cfu) mL⁻¹. 25 µL cell suspension and 5 mL YES culture medium were added into each ampoule. Then, 0, 15, 20, 25, 30, 35, 40 and 45 µL 25.1 mg/mL CuLCl₂ DMSO solutions were also introduced into these ampoules, respectively. Finally, each ampoule which contains the cell suspension of *S. pombe* and the compound was sealed up and placed inside the microca-

lorimeter. After a balance of the instrument, the temperature of ampoules reached 32 °C and the heat-flow power-time (HFP-t) curve was recorded by computer using the Thermometric AB program (Sweden) until the recorder returned to the baseline. All the experiments were maintained at 32 °C. CuCl₂ and **L** were also tested without any antifungal activity. The stability test of CuLCl₂ shows that the absorbance and wavelength of UV absorption spectra of the complex in DMSO solution did not change till 7 days (data not shown).

3 RESULTS AND DISCUSSION

3.1 Synthesis and characterization

The reaction of ethylene diamine and 2-acetylpyrazine in 1:1 M ratio in methanol medium yields a single condensation (**L**). Positive ion mass spectra for the ligand shows peaks related to fragments of the type [LH]⁺ 165.0 and 269.1 *m/z*. This indicates that the ligand was mixed to single condensation and double condensation (269.1 *m/z*). Even after using excessive ethylene diamine, the results are unchanged. Fortunately, it does not affect the copper(II) complex synthesis. When the methanol solution of copper chloride was dropped to chloroform solution of ligand, double condensation copper complex into precipitate was filtered out. Because when the filtrate was volatilized, the powder X-ray diffraction patterns of the crystal agreed very well with the PXRD patterns simulated according to the X-ray single-crystal data, thus indicating that the products were pure phase. The image of the PXRD is presented in Fig. 1.

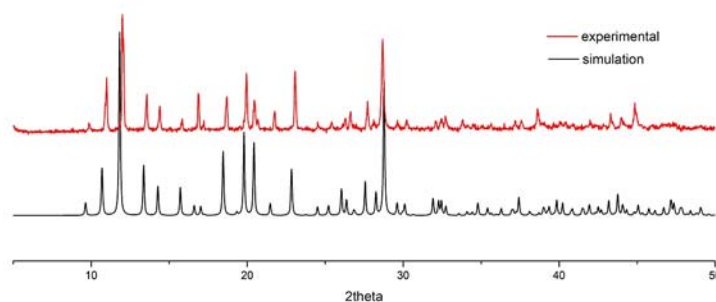


Fig. 1. Simulated and experimental PXRD patterns of complex CuLCl_2 at room temperature

3.2 FTIR spectra

The infrared spectra of the compound exhibit strong absorption at 3290 and 3235 cm^{-1} and it can be assigned, respectively to the asymmetric and symmetric ν_{NH} of the coordinated primary amine in CuLCl_2 , also consistent with a single condensed ligand. The strong and sharp absorptions at 1658 and 1565 cm^{-1} correspond to the stretching mode of $\text{C}=\text{N}$ bond of the Schiff bases ligand, indicating the azomethine N-coordination. The strong and sharp absorptions at 1411 and 1373 cm^{-1} , respectively are attributed to the asymmetric bending vibration of the $-\text{CH}_3$ & $-\text{CH}_2-$ and the symmetric bending vibration of the $-\text{CH}_3$ groups. The $\text{Cu}-\text{N}$ vibrations of the metal-bound Schiff bases are located at 538 , 485 and 454 cm^{-1} . The solid compound is stable in air.

3.3 Crystal structure of CuLCl_2

It crystallizes in the triclinic system, $P\bar{1}$ space group. The molecular structure and selected bond lengths and bond angles related to the coordination environment of the metal are given in Fig. 2 and Table 1. The complex is mononuclear, five-coordinate species. The central copper ion is coordinated by two chlorides and three N atoms. The Schiff bases act as a tridentate chelating ligand, giving two five-membered rings. The coordination geometry of Cu(II) is a distorted squaral pyramid. Atoms $\text{N}(1)$, $\text{N}(3)$, $\text{N}(4)$ and $\text{Cl}(1)$ form the basal plane and atom $\text{Cl}(2)$ is in the apical position. The $\text{Cl}(2)-\text{Cu}(1)-\text{N}/\text{Cl}(1)$ bond angles are from 97.50 to 101.17° . The effect of the chelate rings is clearly

observed in $\text{N}(1)-\text{Cu}(1)-\text{N}(3)$ and $\text{N}(3)-\text{Cu}(1)-\text{N}(4)$ bond angles, which deviate by 11.06 and 8.04° , respectively from the ideal value (90°). As a result, the $\text{N}(1)-\text{Cu}(1)-\text{N}(4)$ axis is not linear ($156.83(10)^\circ$), significantly deviated from the ideal value of 180° . The $\text{Cu}-\text{N}$ distances in the basal plane are $1.981(2)$, $2.016(2)$ and $2.056(2)\text{ \AA}$. The molecules formed a one-dimensional chain through hydrogen bonds ($\text{N}(4)-\text{H}(4\text{A})\cdots\text{Cl}(1)$ $3.415(3)\text{ \AA}$, $140.5(2)^\circ$ and $\text{N}(4)-\text{H}(4\text{B})\cdots\text{Cl}(2)$ $3.438(2)\text{ \AA}$, $138.9(1)^\circ$), and then formed a three-dimensional network by hydrogen bonds ($\text{C}(7)-\text{H}(7\text{A})\cdots\text{Cl}(1)$ $3.520(3)\text{ \AA}$, $128.4(2)^\circ$, $\text{C}(2)-\text{H}(2)\cdots\text{Cl}(2)$ $3.617(4)\text{ \AA}$, $160.5(2)^\circ$, $\text{C}(3)-\text{H}(3)\cdots\text{Cl}(2)$ $3.618(3)\text{ \AA}$, $166.1(2)^\circ$ and $\text{C}(5)-\text{H}(5\text{B})\cdots\text{Cl}(2)$ $3.756(3)\text{ \AA}$, $158.2(2)^\circ$).

3.4 Antifungal activity

Fig. 3 shows the heat power curve of *S. pombe* growth ($P-t$ curve) in the absence of antifungal drugs. In fungi, heat production curves generally have four stages: a lag phase, an exponential growth phase, a stable phase, and a decline. During the exponential growth phase, the following is true of microbes:

$$P_t = P_0 \exp(kt) \quad \text{or} \quad \ln P_t = \ln P_0 + kt \quad (1)$$

P_0 is the thermal power of the exponential growth at the beginning of the growth cycle and P_t is the thermal power of the exponential growth at time t . For different concentrations of antifungal drugs, the growth rate constant k can be determined by entering P_t and t of the exponential growth phase into Equation (1). Then the $\ln P_t-t$ data can be dealt with by linear fitting. In this way, the maximum

metabolic power of exponential growth P_m , the corresponding appearance time t_m , the generation time t_G , the half-inhibitory concentration IC_{50} , the

inhibition rate I , and other parameters can be calculated.

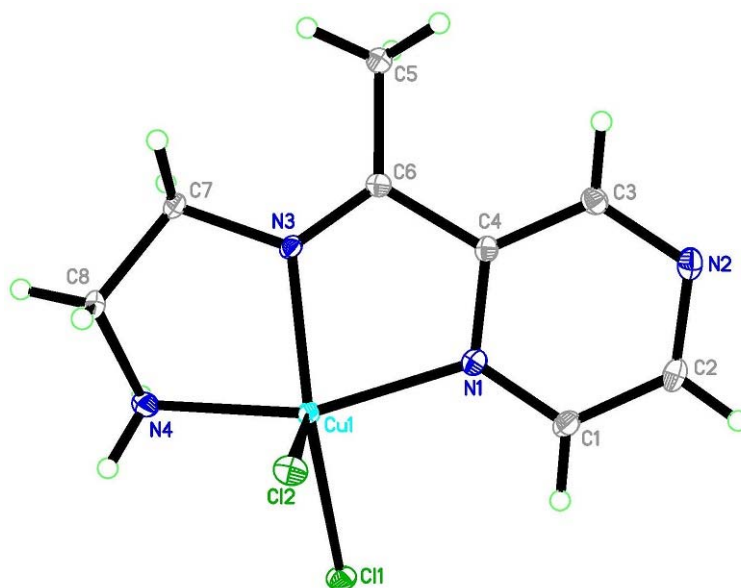


Fig. 2. Structure of $CuLCl_2$. Displacement ellipsoids are drawn at the 30% probability level

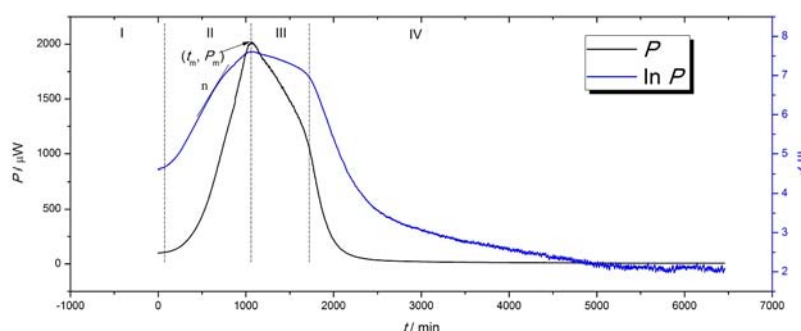


Fig. 3. Metabolic $P-t$ and $\ln P-t$ curves of *S. pombe*. I-lag phase; II-exponential growth phase; III-stable phase; IV-decline phase. The straight line n is the linear fit results of phase II

Here, an equation was used to determine the generation time (t_G):

$$t_G = \ln 2/k \quad (2)$$

At sufficient concentrations, antibiotics can inhibit the microbial growth. The results observed here indicated a constant reduction in the growth rate. In this way, the rate of inhibition (I (%)) can be defined as follows:

$$I = (k_0 - k_c)/k_0 \times 100\% \quad (3)$$

Here, k_0 is the rate constant when cell growth is not inhibited and k_c represents the rate constant at drug concentration C . A drug concentration corres-

ponding to an inhibition rate of 50% is the half-inhibitory concentration IC_{50} ; this parameter can be used to measure the drug sensitivity of bacteria and fungi. The low IC_{50} indicates that the microbes are sensitive to the drug, indicating considerable antifungal activity.

Fig. 4 shows the heat production curves of *S. pombe* growth for different concentrations of $CuLCl_2$. The effect of $CuLCl_2$ on the growth and metabolic activity of *S. pombe* is reflected in the thermal power output curves. The initial point of the thermal power of exponential growth of *S. pombe* in

the CuLCl_2 -treated group goes right along with the increase of CuLCl_2 concentration. It indicates that the CuLCl_2 -treated group had a longer lag phase than the control group. The P_m value and the slope

of the P - t curve decrease along with the increase of CuLCl_2 concentration. It indicates that the growth and metabolism of *S. pombe* had considerable decrease in the presence of CuLCl_2 .

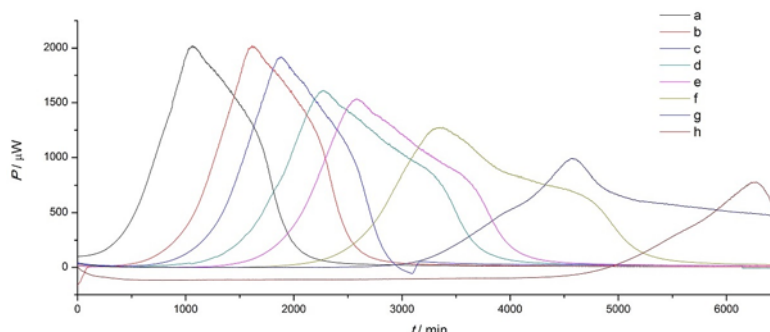


Fig. 4. Heat power curves of *S. pombe* growth under different concentrations of CuLCl_2 . a. 0 $\mu\text{g/mL}$; b. 75.3 $\mu\text{g/mL}$; c. 100.4 $\mu\text{g/mL}$; d. 125.5 $\mu\text{g/mL}$; e. 150.6 $\mu\text{g/mL}$; f. 175.7 $\mu\text{g/mL}$; g. 200.8 $\mu\text{g/mL}$; h. 225.9 $\mu\text{g/mL}$

Table 2 gives the relevant thermodynamic parameters calculated by Eqs. (1), (2) and (3). It showed

that the high concentration of CuLCl_2 considerably slowed the generation time t_G of *S. pombe*.

Table 2. Thermodynamic Parameters of *S. Pombe* under Different Concentrations of CuLCl_2^a

$C(\mu\text{g/mL})$	$t_m(\text{min})$	$P_m(\mu\text{W})$	$k(\times 10^{-6} \text{ min}^{-1})$	$t_G(\text{min})$	$I(\%)$	$IC_{50}(\mu\text{g/mL})$
0	1061.88	2023.21	4180 \pm 1.51	165.82	0.00	
75.3	1615.92	2023.21	4150 \pm 5.03	167.02	0.72	
100.4	1879.73	1918.53	4020 \pm 3.42	172.42	3.83	
125.5	2274.05	1612.88	3960 \pm 4.92	175.03	5.26	
150.6	2582.92	1536.07	3930 \pm 5.04	176.37	5.98	213
175.7	3376.76	1276.47	3480 \pm 4.14	199.18	16.75	
200.8	4567.58	991.39	2600 \pm 8.65	266.59	37.80	
225.9	6232.79	779.32	1520 \pm 2.31	456.01	63.64	

^a The R value for all processing is 0.99.

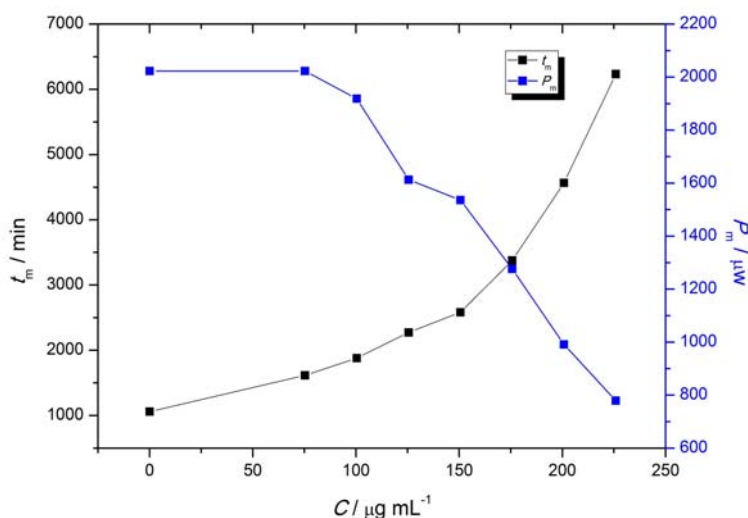


Fig. 5. Relationship between maximum thermal power P_m , the corresponding appearance time t_m with the concentration C of CuLCl_2 . CuLCl_2 : 0, 75.3, 100.4, 125.5, 150.6, 175.7, 200.8 and 225.9 $\mu\text{g/mL}$

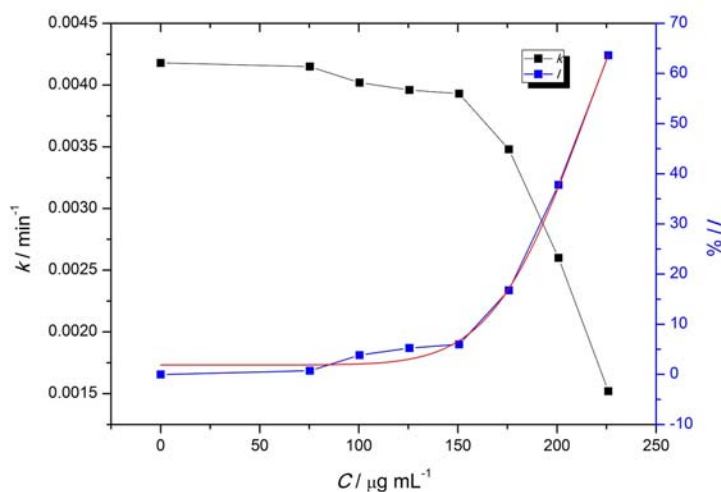


Fig. 6. Relationship between the growth rate constant k , inhibition rate I with the concentration C of CuLCl_2 . CuLCl_2 : 0, 75.3, 100.4, 125.5, 150.6, 175.7, 200.8 and 225.9 $\mu\text{g/mL}$

Figs. 5 and 6 show that the concentration of CuLCl_2 is negatively correlated with the maximum power output P_m and the growth rate constant k of *S. pombe*, and positively related to t_m and the inhibition rate I .

The half-inhibitory concentration, given as IC_{50} ,

$$I = 117.75 + \frac{1.89 - 117.75}{1 + \left(\frac{C}{222.15}\right)^{8.05}}, \quad R = 0.99329$$

Thus, $IC_{50} = 213 \mu\text{g/mL}$. It has a good antifungal activity as some coordination compounds with related N_3CuCl_2 structure^[10, 11, 21-24].

4 CONCLUSION

In this work, we synthesized a novel Schiff base copper complex CuLCl_2 . The central atom copper of the complex has five coordination structures. The

is commonly used to assess the drug sensitivity of the microbes; the “Logistic dose response” fitting inhibition rate I vs. C can be used to determine this parameter (Fig. 6). The relationship between the rate of inhibition and the concentration of CuLCl_2 can be expressed as follows:

antifungal activity of the complex was analyzed from the thermal spectrum of growth and metabolism of *S. pombe* under different concentrations of CuLCl_2 . The growth rate constant, inhibition rates, and the half-inhibitory concentrations of *S. pombe* under different concentrations of CuLCl_2 were obtained. The half-inhibitory concentration IC_{50} shows that the inhibitory abilities of CuLCl_2 on *S. pombe* strain are effective.

REFERENCES

- (1) Almirante, B.; Rodríguez, D.; Park, B. J.; Cuenca-Estrella, M.; Planes, A. M.; Almela, M.; Mensa, J.; Sanchez, F.; Ayats, J.; Gimenez, M.; Saballs, P.; Fridkin, S. K.; Morgan, J.; Rodriguez-Tudela, J. L.; Warnock, D. W.; Pahissa, A. Epidemiology and predictors of mortality in cases of candida bloodstream infection: results from population-based surveillance, barcelona, spain, from 2002 to 2003. *J. Clin. Microbiol.* **2005**, 43, 1829–1835.
- (2) Pfaller, M. A.; Pappas, P. G.; Wingard, J. R. Invasive fungal pathogens: current epidemiological trends. *Clin. Infect. Dis.* **2006**, 43, S3–S14.
- (3) Payne, D. J. Desperately seeking new antibiotics. *Science* **2008**, 321, 1644–1645.
- (4) Kong, W. J.; Wang, J. B.; Xing, X. Y.; Xiao, X. H.; Zhao, Y. L.; Zang, Q. C.; Zhang, P.; Jin, C.; Li, Z. L.; Liu, W. Antifungal evaluation of cholic

- acid and its derivatives on *Candida albicans* by microcalorimetry and chemometrics. *Anal. Chim. Acta* **2011**, 689, 250–256.
- (5) Guo, Q. L.; Zhang, J.; Xu, Z. Q.; Li, R.; Jiang, F. L.; Xiao, Q.; Liu, Y. Comparative study on the effects of two antifungal drugs against *Candida albicans* by microcalorimetry and transmission electron microscopy. *Thermochim. Acta* **2012**, 543, 82–87.
- (6) Buchanan, K.; Murphy, J. What makes *Cryptococcus neoformans* a pathogen? *Emerg. Infect. Dis.* **1998**, 4, 71–83.
- (7) Armstrong-James, D.; Meintjes, G.; Brown, G. D. A neglected epidemic: fungal infections in HIV/AIDS. *Trends Microbiol.* **2014**, 22, 120–127.
- (8) da Silva, C. M.; da Silva, D. L.; Modolo, L. V.; Alves, R. B.; de Resende, M. A.; Martins, C. V. B.; de Fátima, Â. Schiff bases: a short review of their antimicrobial activities. *J. Adv. Res.* **2011**, 2, 1–8.
- (9) Sztanke, K.; Maziarka, A.; Osinka, A.; Sztanke, M. An insight into synthetic Schiff bases revealing antiproliferative activities in vitro. *Bioorg. Med. Chem.* **2013**, 21, 3648–3666.
- (10) Chaviara, A. T.; Cox, P. J.; Repana, K. H.; Pantazaki, A. A.; Papazisis, K. T.; Kortsaris, A. H.; Kyriakidis, D. A.; Nikolov, G. S.; Bolos, C. A. The unexpected formation of biologically active Cu(II) Schiff mono-base complexes with 2-thiophene-carboxaldehyde and dipropylentriamine: crystal and molecular structure of $Cu(dpta)SCl_2$. *J. Inorg. Biochem.* **2005**, 99, 467–476.
- (11) Chaviara, A. T.; Cox, P. J.; Repana, K. H.; Papi, R. M.; Papazisis, K. T.; Zambouli, D.; Kortsaris, A. H.; Kyriakidis, D. A.; Bolos, C. A. Copper(II) Schiff base coordination compounds of dien with heterocyclic aldehydes and 2-amino-5-methyl-thiazole: synthesis, characterization, antiproliferative and antibacterial studies. Crystal structure of $Cu(dien)OOC_2$. *J. Inorg. Biochem.* **2004**, 98, 1271–1283.
- (12) Patil, S. A.; Prabhakara, C. T.; Halasangi, B. M.; Toragalmath, S. S.; Badami, P. S. DNA cleavage, antibacterial, antifungal and anthelmintic studies of Co(II), Ni(II) and Cu(II) complexes of coumarin Schiff bases: synthesis and spectral approach. *Spectrochim. Acta A* **2015**, 137, 641–651.
- (13) Li, C. H.; Song, X. Z.; Jiang, J. H.; Yang, P.; Yao, F. H.; Li, X.; Xiao, S. X.; Xie, J. Q.; Peng, M. N.; Pan, L.; Wu, X. B.; Peng, X.; Tang, C. G.; Zhang, P. H.; Jiang, C.; Liu, W. Q.; Li, Q. G. Synthesis, thermochemical and thermokinetic studies on the mononuclear copper Valen Schiff base complex. *Sci. Sin. Chim.* **2014**, 44, 981–988.
- (14) Jiang, J. H.; Li, X.; Xiao, S. X.; Gu, H. W.; Li, C. H.; Yang, P.; Wei, D. L.; He, D. G.; Li, A. T.; Li, X.; Yao, F. H.; Li, Q. G. Interaction of 2-[[4-amino-5-(3,4,5-trimethoxy-benzyl)-pyrimidin-2-ylimino]-methyl]-6-methoxy-phenol with *S. pombe* Cells and BSA. *Chem. J. Chin. U* **2014**, 35, 831–838.
- (15) Nithya, P.; Simpson, J.; Govindarajan, S. Template synthesis, structural variation, thermal behavior and antimicrobial screening of Mn(II), Co(II) and Ni(II) complexes of Schiff base ligands derived from benzyl carbazate and three isomers of acetylpyridine. *Inorg. Chim. Acta* **2017**, 467, 180–193.
- (16) Liu, X.; Manzur, C.; Novoa, N.; Celedón, S.; Carrillo, D.; Hamon, J. R. Multidentate unsymmetrically-substituted Schiff bases and their metal complexes: synthesis, functional materials properties, and applications to catalysis. *Coord. Chem. Rev.* **2018**, 357, 144–172.
- (17) Pervaiz, M.; Yousaf, M.; Ahmad, I.; Munawar, A.; Saeed, Z.; Adnan, A.; Gulzar, T.; Kirn, S.; Kamal, T.; Ahmad, A. Synthesis, spectral and antimicrobial studies of amino acid derivative Schiff base metal (Co, Mn, Cu, and Cd) complexes. *Spectrochim. Acta A* **2018**, In press.
- (18) Li, X.; Jiang, J. H.; Chen, Q.; Xiao, S. X.; Li, C. H.; Gu, H. W.; Zhang, H.; Hu, J. L.; Yao, F. H.; Li, Q. G. Synthesis of nordihydroguaiaretic acid derivatives and their bioactivities on *S. pombe* and K562 cell lines. *Eur. J. Med. Chem.* **2013**, 62, 605–613.
- (19) Loewith, R.; Hubberstey, A.; Young, D. Skh1, the MEK component of the mkh1 signaling pathway in *Schizosaccharomyces pombe*. *J. Cell Sci.* **2000**, 113, 153–160.
- (20) Brown, J. C. S.; Nelson, J.; VanderSluis, B.; Deshpande, R.; Butts, A.; Kagan, S.; Polacheck, I.; Krysan, D. J.; Myers, C. L.; Madhani, H. D. Unraveling the biology of a fungal meningitis pathogen using chemical genetics. *Cell* **2014**, 159, 1168–1187.
- (21) Ghosh, K.; Kumar, P.; Tyagi, N.; Singh, U. P.; Goel, N.; Chakraborty, A.; Roy, P.; Baratto, M. C. DNA interaction, superoxide scavenging and cytotoxicity studies on new copper(II) complexes derived from a tridentate ligand. *Polyhedron* **2011**, 30, 2667–2677.
- (22) Gokhale, N. H.; Padhye, S. S.; Padhye, S. B.; Anson, C. E.; Powell, A. K. Copper complexes of carboxamidrazone derivatives as anticancer agents. 3. Synthesis, characterization and crystal structure of $[Cu(apcc)Cl_2]$, (apcc = N1-(2-acetylpyridine)pyridine-2-carboxamidrazone). *Inorg. Chim. Acta* **2001**, 319, 90–94.
- (23) Primik, M. F.; Göschl, S.; Jakupec, M. A.; Roller, A.; Keppler, B. K.; Arion, V. B. Structure-activity relationships of highly cytotoxic copper(II) complexes with modified indolo[3,2-c]quinoline ligands. *Inorg. Chem.* **2010**, 49, 11084–11095.
- (24) Primik, M. F.; Mühlgassner, G.; Jakupec, M. A.; Zava, O.; Dyson, P. J.; Arion, V. B.; Keppler, B. K. Highly cytotoxic copper(II) complexes with modified paullone ligands. *Inorg. Chem.* **2010**, 49, 302–311.